
FOR THE RECORD

Direct measurement of islet amyloid polypeptide fibrillogenesis by mass spectrometry

JENNIFER L. LARSON, ERIC KO, AND ANDREW D. MIRANKER

Department of Molecular Biophysics and Biochemistry, Yale University, 260 Whitney Avenue, P.O. Box 208114,
New Haven, Connecticut 06520

(RECEIVED September 23, 1999; FINAL REVISION December 3, 1999; ACCEPTED December 3, 1999)

Abstract: A novel method for monitoring fibrillogenesis is developed and applied to the amyloidogenic peptide, islet amyloid polypeptide (IAPP). The approach, based on electrospray ionization mass spectrometry, is complementary to existing assays of fibril formation as it monitors directly the population of precursor rather than product molecules. We are able to monitor fiber formation in two modes: a quenched mode in which fibril formation is halted by dilution into denaturant and a real time mode in which fibril formation is conducted within the capillary of the electrospray source. Central to the method is the observation that fibrillar IAPP does not compromise the ionization of monomeric IAPP. Furthermore, under mild ionization conditions, fibrillar IAPP does not dissociate and contribute to the monomeric signal. Critically, we introduce an internal standard, rat IAPP, for analysis on the mass spectrometer. This standard is sufficiently similar in sequence in that it ionizes identically to human IAPP. Furthermore, the sequence is sufficiently different in that it does not form fibrils and is distinguishable on the basis of mass. Applied to IAPP fibrillogenesis, our technique reveals that precursor consumption in seeded reactions obeys first-order kinetics. Furthermore, a consistent level of monomer persists in both seeded and unseeded experiments after the fibril formation is complete. Given the inherent stability of fibrils, we expect this approach to be applicable to other amyloid systems.

Keywords: amylin; amyloid; electrospray; fibrillogenesis; islet amyloid polypeptide; mass spectrometry; protein folding; type II diabetes

Amyloid plaque deposition is the hallmark of an increasing number of clinical conditions including Alzheimer's disease, type II diabetes, and transmissible spongiform encephalopathies (Kelly,

Reprint requests to: Andrew D. Miranker, Department of Molecular Biophysics and Biochemistry, Yale University, 260 Whitney Avenue, P.O. Box 208114, New Haven, Connecticut 06520; e-mail: Andrew.Miranker@yale.edu.

Abbreviations: IAPP, islet amyloid polypeptide; ESI-MS, electrospray ionization mass spectrometry; HFIP, hexafluoroisopropanol; hIAPP, human islet amyloid polypeptide; rIAPP, rat islet amyloid polypeptide; GuHCl, guanidine hydrochloride.

1998). The predominant component of these plaques is unbranched protein fibers formed from a normally soluble precursor. From a biophysical standpoint, this problem is particularly fascinating as proteins that are apparently unrelated in sequence and in their native conformations aggregate into fibrils with common structural and histological features (Sunde et al., 1997). These features include a crossed- β -sheet organization in which the β -strands are arranged perpendicular to the fibril axis, and the display of green birefringence upon binding of the dye Congo red. Recently, a number of proteins, e.g., SH3 homology domain of PI3 kinase (Guijarro et al., 1998), have been identified that can be induced to form amyloid fibrils, but do not have clinical consequences. This suggests that fibril formation may be a general physical property of polypeptides under appropriate conditions (Chiti et al., 1999).

We are engaged in the study of diabetes-related amyloid. In 90% of post-mortem patients diagnosed with type II (noninsulin dependent) diabetes, amyloid plaques are found in the pancreas (Kahn et al., 1999). The main component of the plaques is a fibrillar form of islet amyloid polypeptide (IAPP), a 37 residue C-terminally amidated peptide hormone, co-secreted with insulin by the β -cells of the pancreas (Cooper et al., 1987). The plaques contribute significantly to the pathogenesis of the ailment as they are associated with β -cell dysfunction. Indeed, β -cell mass is significantly reduced in diabetic patients, and recent work has shown that IAPP fibrils produced in vitro are cytotoxic to cultured β -cells (Lorenzo et al., 1994).

As in protein folding, an understanding of the process of fibrillogenesis requires that the structure, kinetics, and stabilities of all components of the pathway be characterized. However, this is extremely problematic in amyloid research for several reasons (Harper & Lansbury, 1997). First, the order of the reaction is very high, causing the kinetics to be extremely sensitive to small variations in precursor concentration. Second, the process occurs via a nucleation-dependent polymerization pathway, characterized by an initial lag phase followed by a growth phase. It is not uncommon for the growth-phase kinetics of fibril formation to be rapid in comparison to the lag phase of fibril formation.

A number of powerful methods have been developed for monitoring the kinetics of fibril formation. These include, for example, the binding of histological dyes (Kudva et al., 1998), light scattering (Lomakin et al., 1996), and atomic force microscopy

(Goldsbury et al., 1999). In this paper, we develop and exploit electrospray ionization mass spectrometry (ESI-MS) for the direct measurement of IAPP amyloid formation. This approach differs fundamentally from others in that it monitors directly the consumption of precursor, as opposed to observing the formation of end product. We have used this technique to measure fibril formation kinetics in real time and measured the concentration of monomeric IAPP after fibrillogenesis is apparently complete.

Results: Measurement of hIAPP concentration by ESI-MS: Our ability to monitor fibrillogenesis kinetics relies on accurate measurement of the concentration of free IAPP under a variety of solution conditions. One would not normally use mass spectrometry for such a measurement as the efficiency of electrospray ionization of a protein is dependent on instrumentation, solution conditions, and the primary sequence (Loo, 1997). Therefore, it is not possible to accurately determine the solution concentration of a protein directly from the number of ions measured on the mass spectrometer. We investigated the use of internal standards (in the ionized solution) to accurately determine an unknown protein concentration. Previously, it was demonstrated that a protein differing only in isotopic distribution may be used as an internal standard in pulse labeling hydrogen deuterium exchange experiments (Hooke et al., 1995). Here, we have investigated the extent to which variations in protein sequence affect ionization efficiency with a view toward concentration determination. For our purposes, a suitable standard must differ in mass and should not interact with the protein being studied.

IAPP from rat (rIAPP) is desirable as an internal standard for fibrillogenesis studies of human IAPP (hIAPP) as it is not fibrillogenic (Westermarck et al., 1990). rIAPP and hIAPP differ by a total of six amino acids; these include the substitution of an alanine and two serine residues in hIAPP for three proline residues within the proposed amyloidogenic core (20–29). This gives rise to a mass difference of 17 Da, which is trivially resolved on our instrumentation (Fig. 2B). hIAPP and rIAPP stock solutions were mixed in varying proportions with either denaturing (50% CH₃CN, 0.2% formic acid) or physiological buffer (1 mM Tris pH 7.4, 50 mM ammonium acetate) and mass analyzed. The ratio of the total number of ions measured on the mass spectrometer was plotted against the ratio of the solution concentration (Fig. 1). The stock solution concentrations were confirmed by amino acid analysis. Under both conditions, the relative total ion count and the relative solution concentrations correlated nearly 1:1. As the correlation is 1:1 under a variety of solution conditions and is tolerant of minor variations in instrumentation conditions we can determine the solution concentration of hIAPP by addition of a known amount of rIAPP.

Extension of this approach was also assessed for unrelated proteins. Hen lysozyme and hIAPP were mixed in varying proportions and mass analyzed. These two proteins differ in mass by 10 kDa (14 kDa vs. 4 kDa, respectively). Given that these two proteins have unrelated sequences, it is remarkable that there is a correlation between the relative solution concentration and the relative number of ions measured (Fig. 1). It is possible, therefore, to use an arbitrary protein as an internal standard for the measurement of concentration of another protein. This, however, requires the prior determination of a standard curve to establish a region of linearity between the relative solution concentrations and ion counts.

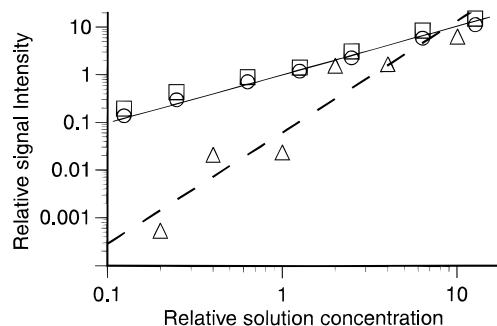


Fig. 1. Standard curves of the integrated relative peak intensities measured by ESI-MS vs. the relative solution concentrations. Δ represents hIAPP: hen lysozyme ratios. Protein was ionized from 50 mM ammonium acetate buffer pH 3. Lysozyme concentration was kept at 2.5 μ M while the hIAPP concentration was varied. The dotted line is a best linear fit to the data. \square, \circ represent hIAPP:rIAPP ratios. Total protein concentration was kept to $\sim 20 \mu$ M. Protein was sprayed either from 50% CH₃CN, 0.2% formic (\square) or 1 mM Tris buffer pH 7.4, 50 mM ammonium acetate (\circ). A solid line is drawn at a correlation of 1:1.

Measurement of hIAPP monomer concentration in mixed monomer/fibril solutions: Monitoring fibrillogenesis by mass spectrometry through kinetic and equilibrium experiments rests on the ability to quantitate the concentration of nonfibrillar IAPP. Mass analysis of noncovalent complexes typically results in dissociation and the separate measurement of individual components (Loo, 1997). If fibrils dissociated upon ionization, neither kinetic nor equilibrium measurements would be possible by this method. Recent advances in electrospray ionization, however, now permit ionization under sufficiently mild conditions that noncovalent complexes including hIAPP fibrils remain intact. Using a fluorescence assay, we have found that a solution of 50 μ M hIAPP forms fibrils in minutes under physiological conditions (Fig. 2A) (Kudva et al., 1998). After completion of the reaction, the addition of rIAPP to 1 μ M results in a mass spectrum with near equal intensity for hIAPP and rIAPP peaks (Fig. 2B). Since hIAPP and rIAPP ionize with near identical efficiency under these conditions (Fig. 1), this implies that monomeric hIAPP is present in solution to $\sim 1 \mu$ M and that fibrillar hIAPP contributes only fractionally to the monomeric signal, if at all.

To quantitate the extent to which fibrils contribute to the ESI-MS monomeric signal, the sample was filtered using a centrifugal filtration device with a 100 kDa molecular weight cutoff. The proportion of rIAPP to hIAPP in the filtrate measured by ESI-MS is not significantly altered (Fig. 2C). There is, however, a complete elimination of fibril signal (Fig. 2A) in the filtrate while enhancement of ThT fluorescence at 447 nm is correspondingly stronger in the filtration retentate (Fig. 2A). Repeat analysis of the change in apparent monomer concentration before and after filtration suggests that a maximum of $2 \pm 2\%$ of the monomer signal is derived from fiber. This strongly suggests that hIAPP fibrils do not contribute to the monomeric hIAPP signal measured by ESI-MS.

Kinetics of IAPP amyloid formation: hIAPP amyloid formation was analyzed over time using the ThT fluorescence assay (Fig. 3), revealing kinetics consistent with the nucleation-dependent polymerization model. Under our fibrillogenesis conditions at 25 μ M, hIAPP displays a 5–10 min lag phase followed by a rapid elonga-

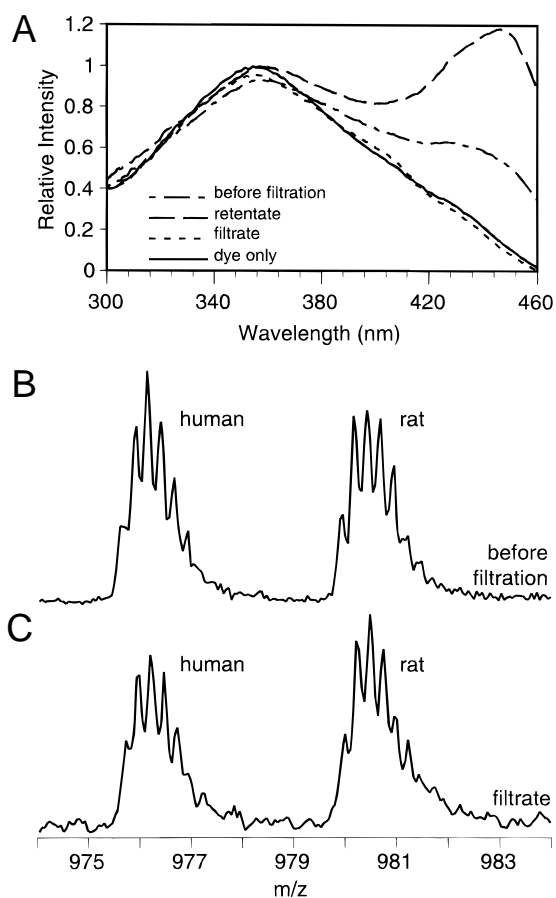


Fig. 2. A fibril-monomer mixture yields only monomer signal by ESI-MS. hIAPP fibrils were prepared at $50 \mu\text{M}$ as described and incubated for 30 min. The solution was then diluted 1:1 into 80% acetonitrile/0.32% formic acid, containing $2 \mu\text{M}$ rIAPP. This solution was assayed for the presence of fibrils using the ThT binding assay (A, ---). The fluorescence excitation spectrum shows a maximum at 447 nm. **B:** ESI-MS of the same solution yields near equal intensities for hIAPP and rIAPP. The solution was then filtered using a 100 kDa cutoff membrane (Microcon 100, Amicon) and assayed for fibrils using the ThT binding assay. The filtrate shows no enhanced fluorescence at 447 nm (A, ---), while the retentate shows a corresponding increase (A, —), suggesting efficient separation of fibril from monomer. ESI-MS of the filtrate (C) gives relative intensities for hIAPP:rIAPP which are unchanged by comparison to the unfiltered sample (B).

tion phase. Furthermore, this lag phase may be bypassed by the introduction of $2 \mu\text{M}$ (monomer concentration) of fibrils (Fig. 3). Fibrils used for seeding were freshly prepared at $50 \mu\text{M}$ under matched conditions.

We have capitalized on the stability of fibrils to electrospray ionization to measure fibril formation by monitoring the consumption of precursor. An hIAPP stock solution was diluted to $50 \mu\text{M}$ in physiological buffer. Under these conditions, a $50 \mu\text{M}$ solution of hIAPP displays a lag phase of 30–90 s as measured using the ThT fluorescence assay (data not shown). At a series of time points, aliquots are quenched by 1:10 dilution into 50% CH_3CN , 0.2% formic acid containing $5 \mu\text{M}$ rIAPP. The kinetics of fibril formation can clearly be seen as the loss of hIAPP peak intensity relative to the rat internal standard (Fig. 4).

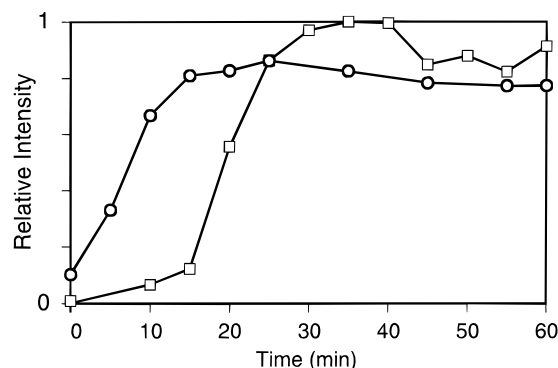


Fig. 3. The effects of seeding on fibrillogenesis. \square , IAPP was diluted to $25 \mu\text{M}$ in pH 7.4 buffer. Aliquots were removed at successive time points and assayed for fibril formation by ThT binding. \circ , IAPP was diluted to $25 \mu\text{M}$ in the same refolding buffer used for \square except for the addition of $2 \mu\text{M}$ (in monomer units) IAPP fibrils. Fibrils for seeding had been prepared from a $50 \mu\text{M}$ fibril-forming reaction under matched conditions.

The ability to seed hIAPP with preformed fibrils allows us to overwhelm spontaneous and nonspecific nucleation (Harper & Lansbury, 1997) and measure separately the elongation phase of this reaction. We capitalized on this to study the elongation kinetics of hIAPP fibrillogenesis in real time by mass spectrometry (Fig. 5). At time zero, hIAPP was diluted from HFIP stock solution to $25 \mu\text{M}$ in aqueous buffer at pH 7.4, containing $2 \mu\text{M}$ (monomer units) of hIAPP fibrils and $2 \mu\text{M}$ rIAPP as tracer. The solution was immediately loaded into a capillary, mounted in the source, and data were acquired directly from the aqueous reaction mixture rather than as discrete time points quenched in organic solvent.

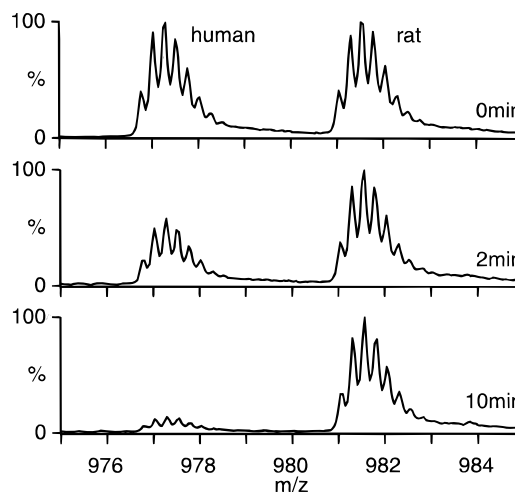


Fig. 4. ESI-MS spectra of hIAPP monomer at selected time points after initiation of fibrillogenesis. hIAPP was diluted from a 1 mM stock solution in HFIP, to a final concentration of $50 \mu\text{M}$ in 150 mM ammonium acetate, 1 mM Tris, pH 7.4. At each time point, an aliquot was taken from the reaction mixture and diluted to a final concentration of $5 \mu\text{M}$ hIAPP in 50% CH_3CN , 0.2% formic acid, also containing $5 \mu\text{M}$ rIAPP. Over time, the peak intensity of hIAPP decreases compared to rIAPP, representing the consumption of monomer due to amyloid formation.

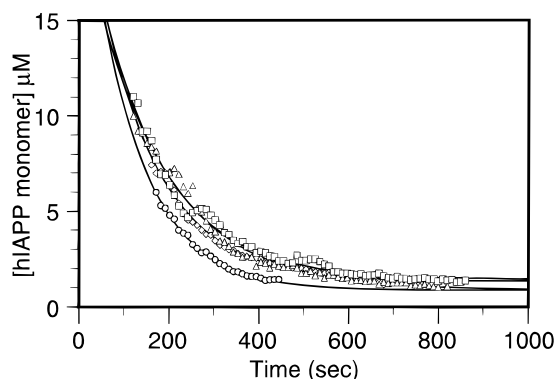


Fig. 5. hIAPP fibril elongation in real-time by ESI-MS. hIAPP was diluted from stock solution in HFIP to $25 \mu\text{M}$ in 150 mM ammonium acetate, 1 mM Tris pH 7.4 in the presence of $2 \mu\text{M}$ (in monomer units) of pre-formed fibrils and $2 \mu\text{M}$ rIAPP to act as the internal standard. The sample was then loaded into the nanospray source and data were acquired in 10 s intervals. Four independent experiments are shown. The data were fit to a single exponential ($A * \exp(-t/B) + C$). The average values and standard deviations of the fits are: $A = 22 \pm 1.8$, $B = 140 \pm 24$, $C = 1.1 \pm 0.3$.

The transfer time to the mass spectrometer results in a dead time of ~ 120 s. In these seeded reactions, no lag time was observed. Indeed, back extrapolation of the first-order kinetics to time zero suggests a concentration of $22 \pm 1.8 \mu\text{M}$, a value in excellent agreement with the estimated starting concentration. The reaction was reproducible permitting multiple reactions to be combined to give an elongation time constant of 140 ± 24 s. Also, we note that the decay in signal is described well by a single exponential and that the endpoint has a value of $1.1 \pm 0.3 \mu\text{M}$. This provides a direct measure of the residual monomer concentration at the end of the reaction.

Discussion: The reaction order for nucleation and elongation of amyloid fibrils is high (Harper & Lansbury, 1997). For example, estimates based on light scattering for $A\beta$ peptide from Alzheimer's disease are 15–70 (Lomakin et al., 1996). As a result, what generally constitutes typical manipulation error (e.g., 1% for pipetting) or concentration determination error (10%) can be amplified into highly irreproducible results. Our development of an internal standard for use in mass spectrometry has therefore served two purposes. First, to rapidly measure an unknown concentration, and second, as an internal correction for manipulation and instrumentation errors.

The concentration of a stock solution of internal standard may be determined to high accuracy, e.g., by repeated amino acid analysis. This stock may then be introduced into a solution of a different protein at unknown concentration for assessment by ESI-MS. This approach has a number of advantages. First, it is rapid, taking only a couple of minutes. Second, it uses a minimal amount of sample. One microliter of a $1 \mu\text{M}$ sample is trivially assessed. In the case of hIAPP, this corresponds to 4 ng, three orders of magnitude less than a typical amino acid analysis. Third, a standard curve is unnecessary for proteins with similar ionization efficiencies. Fourth and uniquely, it is insensitive to heterogeneity either in the form of contaminants or deliberately introduced components. Provided the additional elements in the mixture have distinct masses, the unknown concentration can be accurately determined.

Correlation coefficients for rIAPP vs. hIAPP standard curves are universally very high (Pearson's $r > 0.99$). Furthermore, the average slope of these curves is 1.0 ± 0.2 (standard deviation, $n = 5$). We infer, therefore, that the ionization efficiency of hIAPP and rIAPP are nearly identical. Our choice of rIAPP as an internal standard in this study is based on function, namely that rIAPP does not form fibrils. This use of mass spectrometry, however, is not limited to amyloidosis studies. In such cases, the use of a more closely matched sequence, or an identical sequence with isotopic substitutions (Hooke et al., 1995), would undoubtedly yield further refinement in the accuracy of this approach for concentration determination.

Amyloid fibrils are typically resistant to dissolution even in organic solvents and chaotropic salts. Indeed, hIAPP has been reported to form amyloid in 6 M GuHCl (Kayad et al., 1999). The only reliable way to completely solubilize hIAPP fibrils is by treatment with 70% formic acid (Cooper et al., 1987). While a number of oligomeric systems have demonstrated the maintenance of noncovalent complexes in the gas phase (Loo, 1997), none of these systems demonstrate the extreme stability of an amyloid fibril. Therefore, it is not surprising that a mixture of fibril and monomer yields signal only from the monomeric component. As the high stability of the fibrillar form is common among amyloid systems (Harper & Lansbury, 1997), we expect this observation and our approach to be generally applicable.

We are able to capitalize on the resistance of IAPP fibrils to dissociation in two complementary ways. The first method involves the removal of aliquots from a fibril-formation reaction at discrete time points, which are then quenched by the addition of denaturant and ionized (Fig. 4). The second method employs direct ionization of the amyloid forming solution (Fig. 5). The former readily permits a wide range of time scales, protein concentrations, temperatures, and solution conditions to be explored. The latter permits a high sampling rate and therefore a more rigorous assessment of the kinetic pathways. In both cases, we are measuring a monomeric signal; however, it is possible that the monomeric signal contains contributions from oligomeric intermediates. We do not observe IAPP oligomers under the conditions used in these experiments. This indicates that nonfibrillar oligomers or less stable protofilament intermediates are either present in low abundance, or else are dissociated either by the addition of CH_3CN or by the ionization process.

Kinetics were obtained by seeding the reaction through the addition of pre-formed fibrils. The potential for change in molar fibril concentration derives from either nucleation of new fibers or fragmentation of existing fibrils. The kinetics, however, clearly fit to a single exponential (Fig. 5). Furthermore, as no lag phase is observed and the first-order kinetics extrapolate to near the starting concentration of monomer, this indicates that no new fibril formation is taking place. Clearly under these conditions, the exogenous fibrils are only being elongated. This is similar to observations of $A\beta$ elongation of both ex vivo and synthetic $A\beta$ fibrils (Esler et al., 1997). For the quenched and real-time fibril formation experiments performed here, the concentration of hIAPP monomer at the completion of the measured kinetics is consistently $\sim 1 \mu\text{M}$. We anticipate that both the kinetics of monomer consumption and the residual monomer concentration will be important diagnostics for distinguishing between alternative fibrillogenic pathways. More generally, this approach opens a vital avenue to understanding amyloidosis. As fibril formation is nucleation dependent, one or more intermediates must be present on any fibrillogenic pathway.

Existing methods for measuring kinetics monitors formation of the end product. As our method complements this by directly monitoring consumption of precursor, it is our expectation that a far richer characterization of fibrillogenesis will be achieved.

Materials and methods: *Materials:* Solvents and buffers were purchased from J.T. Baker (Phillipsburg, New Jersey) or Aldrich (Milwaukee, Wisconsin) and were of high-performance liquid chromatography (HPLC) grade. Additionally, hexafluoroisopropanol (HFIP) was further purified by fractional distillation (59–60 °C). Thioflavin T was purchased from Acros (Geel, Belgium). Rat IAPP was obtained from Bachem (King of Prussia, Pennsylvania) and recrystallized hen lysozyme from Boehringer Mannheim (Mannheim, Germany). Human IAPP was synthesized by standard Fmoc solid phase methods and purified in-house by reverse-phase HPLC. Concentration of IAPP peptide stock solutions was determined in-house by amino acid analysis. Molar concentrations of fibril solutions are expressed in monomer units.

Mass spectrometry: Mass spectra were collected using a Micro-mass LCT electrospray time of flight spectrometer. Atmospheric pressure ionization was performed using borosilicate capillaries drawn and sputter coated in-house using a Mo/Au target. To eliminate possible cross-contamination, a fresh needle was used for every sample, and disposable pipette tips were used to load the capillary. All spectra shown are the +4 charge state. Spectra were collected over a mass range of 200–2,500 m/z or 200–5,000 m/z . Signals were typically averaged for 10 s to 1 min with no post-acquisition smoothing or calibration applied. The mass spectrometer ionization source temperature was kept at room temperature.

Formation of IAPP fibrils: Stock solutions of hIAPP were prepared at 1 mM in HFIP. In our hands and others (Kayed et al., 1999), IAPP stock solutions made in HFIP do not form fibrils even at mM concentrations and months of storage. We note that lyophilized peptide stored at –20 °C can nevertheless form unidentified aggregates that are apparently insoluble in HFIP. All of our stocks are made from freshly re-purified (RP-HPLC) peptide. Fibrils are formed by dilution of IAPP from HFIP to 25 or 50 μM in 1 mM Tris, pH 7.4, 150 mM ammonium acetate at room temperature. Formation of fibrils was confirmed by electron microscopy (data not shown). Seeded reactions were achieved after adding 2 μM (monomer units) of pre-formed fibrils at time zero, obtained from a previous 50 μM fibril-formation reaction under the same conditions.

ThT binding assay: Fibril solutions were diluted to 0.25 or 0.50 μM (monomer units) and 5 μM ThT in 50 mM glycine/NaOH buffer pH 9.0. Fluorescence excitation spectra were collected on a Hitachi F-4500 fluorescence spectrophotometer with slit widths of 10 nm

and emission monochromator at $\lambda_{em} = 484$ nm. Enhanced absorbance of ThT was detected at $\lambda_{ex} = 447$ nm, indicating the presence of fibrils (LeVine, 1993). After subtracting the absorbance of ThT in the absence of hIAPP, the data were normalized.

Acknowledgments: This work was supported in part by a grant from the Pew charitable trusts (PO219SC). J.L.L. receives support from an NIH training grant (5T32GM07223). A.D.M. is a Pew scholar in the biomedical sciences. We thank Prof. A. Brünger for use of his fluorimeter. We also thank Dr. C. Morgan for thoughtful comments during preparation of this manuscript.

References

- Chiti F, Webster P, Taddei N, Clark A, Stefani M, Ramponi G, Dobson CM. 1999. Designing conditions for in vitro formation of amyloid protofilaments and fibrils. *Proc Natl Acad Sci USA* 96:3590–3594.
- Cooper GJS, Willis AC, Clark A, Turner RC, Sim RB, Reid KBM. 1987. Purification and characterization of a peptide from amyloid-rich pancreases of type-2 diabetic-patients. *Proc Natl Acad Sci USA* 84:8628–8632.
- Esler WP, Stimson ER, Ghilardi JR, Felix AM, Lu YA, Vinters HV, Mantyh PW, Maggio JE. 1997. A beta deposition inhibitor screen using synthetic amyloid. *Nat Biotechnol* 15:258–263.
- Goldsbury C, Kistler J, Aebi U, Arvinte T, Cooper GJ. 1999. Watching amyloid fibrils grow by time-lapse atomic force microscopy. *J Mol Biol* 285:33–39.
- Guijarro JI, Sunde M, Jones JA, Campbell ID, Dobson CM. 1998. Amyloid fibril formation by an SH3 domain. *Proc Natl Acad Sci USA* 95:4224–4228.
- Harper JD, Lansbury PT Jr. 1997. Models of amyloid seeding in Alzheimer's disease and scrapie: Mechanistic truths and physiological consequences of the time-dependent solubility of amyloid proteins. *Annu Rev Biochem* 66:385–407.
- Hooke SD, Eyles SJ, Miranker A, Radford SE, Robinson CV, Dobson CM. 1995. Cooperative elements in protein-folding monitored by electrospray-ionization mass-spectrometry. *J Am Chem Soc* 117:7548–7549.
- Kahn SE, Andrikopoulos S, Verchere CB. 1999. Islet amyloid: A long-recognized but underappreciated pathological feature of type 2 diabetes. *Diabetes* 48:241–253.
- Kayed R, Bernhagen J, Greenfield N, Sweimeh K, Brunner H, Voelter W, Kapurniotu A. 1999. Conformational transitions of islet amyloid polypeptide (IAPP) in amyloid formation in vitro. *J Mol Biol* 287:781–796.
- Kelly JW. 1998. The alternative conformations of amyloidogenic proteins and their multi-step assembly pathways. *Curr Opin Struct Biol* 8:101–106.
- Kudva YC, Mueske C, Butler PC, Eberhardt NL. 1998. A novel assay in vitro of human islet amyloid polypeptide amyloidogenesis and effects of insulin secretory vesicle peptides on amyloid formation. *Biochem J* 331:809–813.
- LeVine H 3rd. 1993. Thioflavine T interaction with synthetic Alzheimer's disease beta-amyloid peptides: Detection of amyloid aggregation in solution. *Protein Sci* 2:404–410.
- Lomakin A, Chung DS, Benedek GB, Kirschner DA, Teplow DB. 1996. On the nucleation and growth of amyloid beta-protein fibrils—Detection of nuclei and quantitation of rate constants. *Proc Natl Acad Sci USA* 93:1125–1129.
- Loo JA. 1997. Studying noncovalent protein complexes by electrospray ionization mass spectrometry. *Mass Spectrom Rev* 16:1–23.
- Lorenzo A, Razzaboni B, Weir GC, Yankner BA. 1994. Pancreatic-islet cell toxicity of amylin associated with type-2 diabetes-mellitus. *Nature* 368:756–760.
- Sunde M, Serpell LC, Bartlam M, Fraser PE, Pepys MB, Blake CCF. 1997. Common core structure of amyloid fibrils by synchrotron X-ray diffraction. *J Mol Biol* 273:729–739.
- Westermarck P, Engstrom U, Johnson KH, Westermarck GT, Betsholtz C. 1990. Islet amyloid polypeptide: Pinpointing amino acid residues linked to amyloid fibril formation. *Proc Natl Acad Sci USA* 87:5036–5040.